All-or-None versus Graded: Single-Vesicle Analysis Reveals Lipid Composition Effects on Membrane Permeabilization

Beatriz Apellániz,[†‡] José L. Nieva,[†‡] Petra Schwille,[§] and Ana J. García-Sáez[¶‖*]

[†]Unidad de Biofísica, Consejo Superior de Investigaciones Científicas/University of the Basque Country, Bilbao, Spain; [‡]Departamento de Bioquímica, Universidad del País Vasco, Bilbao, Spain; [§]Biophysics, Biotechnologisches Zentrum der Technische Universität Dresden, Dresden, Germany; and [¶]Max Planck Institute for Metals Research and [‖]German Cancer Research Center, BioQuant, Heidelberg, Germany

ABSTRACT We report a single-vesicle approach to compare the all-or-none and graded mechanisms of lipid bilayer permeabilization by CpreTM and NpreTM, two peptides derived from the membrane-proximal external region of the HIV fusion glycoprotein gp41subunit. According to bulk requenching assays, these peptides permeabilize large unilamellar vesicles via all-or-none and graded mechanisms, respectively. Visualization of the process using giant unilamellar vesicles shows that the permeabilization of individual liposomes by these two peptides differs in kinetics, degree of dye filling, and stability of the permeabilized state. All-or-none permeabilization by CpreTM is characterized by fast and total filling of the individual vesicles. This process is usually accompanied by the formation of stably open pores, as judged from the capacity of the vesicles to incorporate a second dye added after several hours. In contrast, graded permeabilization by NpreTM is transient and exhibits slower kinetics, which leads to partial filling of the individual liposomes. Of importance, quantitative analysis of vesicle population distribution allowed the identification of mixed mechanisms of membrane permeabilization and the assessment of cholesterol effects. Specifically, the presence of this viral envelope lipid increased the stability of the permeating structures, which may have implications for the fusogenic activity of gp41.

INTRODUCTION

Biological membranes act as permeability barriers that define the cell and its internal compartments or organelles. They organize into continuous lipid bilayer sheets that exhibit low permeability to polar molecules. However, also essential to life is the ability of cells to exchange matter, information, and energy across their membranes. For this purpose, proteins that act as receptors, channels, or transporters are embedded in biological membranes (1). Other cellular processes also involve the regulated alteration of membrane continuity, as in the case of membrane fusion during vesicle trafficking or the permeabilization of the outer mitochondrial membrane during apoptosis (2,3). In addition, uncontrolled membrane permeabilization can have dramatic consequences for the cell because it can provoke the alteration of ionic homeostasis, leading to the disruption of electrochemical gradients and cell death. Taking advantage of this, organisms ranging from bacteria to mammals have developed a type of self-defense toxins, known as pore-forming proteins or peptides (PFPs), that are secreted to induce the opening of pores in the membranes of pathogens, thus causing their death (4). This strategy is also exploited for therapeutic applications, such as the development of PFP-based antibiotics or the design of membrane-permeabilizing drugs that selectively kill cancer cells (5,6). For these reasons, it is important to understand the molecular mechanisms involved in membrane permeabilization.

Although the molecular mechanism of membrane permeabilization by PFPs remains controversial, several models have been proposed based on structural or kinetic observations (7–13). Depending on the lysis mode, the mechanisms of PFPs are classified as all-or-none or graded (14). On the one hand, the all-or-none mechanism is characterized by strong cooperativity in membrane permeabilization. In addition, the lifetime and/or size of the pore state are large enough to ensure equilibration of the vesicle contents with the external medium. A peptide corresponding to helix 5 of Bax is an example of all-or-none behavior (15,16). On the other hand, the leakage process for graded PFPs leads to partial release of the vesicles contents, and in many cases (but not always (17)), full permeabilization is not easy to achieve, even with high peptide loads on the membrane. The molecular mechanism behind this process is less understood. Current hypotheses consider transient alterations of the membrane permeability that are associated with lipid/polypeptide rearrangements occurring during PFP insertion into the lipid bilayer (7). Another possibility is that transient pores form due to the increase in membrane tension that occurs upon asymmetric binding of the PFP (10). In any case, the graded permeabilization of the lipid bilayer is postulated to occur because the lifetime and small size of the membrane lesions do not allow for equilibration with the external solution.

So far, the classification of all-or-none versus graded mechanisms of membrane permeabilization has been based mainly on in vitro assays (e.g., the ANTS/DPX requenching assay (14,18–21)) of contents release from large unilamellar vesicles (LUVs). Recently, a new method based on analysis

Submitted July 16, 2010, and accepted for publication September 13, 2010.

*Correspondence: ajegarsa@mf.mpg.de

Editor: William C. Wimley.

0006-3495/10/12/3619/10 $2.00

doi: 10.1016/j.bpj.2010.09.027

of the fluorescence lifetime of calcein leakage from LUVs allowed the simultaneous quantification of efflux and graded or all-or none release (22). Although they are generally valid for an initial discrimination between mechanisms, these bulk methods do not allow assessment of solute-encapsulation heterogeneities that may exist in the population of permeabilized vesicles. Consequently, it is difficult to accurately distinguish mixed mechanisms in a sample, i.e., when part of the vesicles are permeabilized in an all-or-none and part in a graded fashion for a given lipid composition and in the presence of a given PFP. As a result, the underlying differences between PFPs that follow all-or-none and graded mechanisms remain poorly characterized. Moreover, the interplay between polypeptide sequence and membrane composition in the mechanism of membrane permeabilization is far from understood.

To gain insight into the all-or-none versus graded mechanisms of membrane permeabilization and directly observe these processes, we developed a single-vesicle approach. Giant unilamellar vesicles (GUVs) are emerging as powerful model systems for investigating membrane permeabilization mechanisms at the individual-vesicle level. The kinetics of single-vesicle leakage, individual-vesicle integrity during permeabilization, and the effects of lipid-phase coexistence can be successfully addressed with this approach (23–27). In this study, we compared the kinetics, stability of the permeabilized state, and degree of individual vesicle permeabilization for two membrane-active peptides, CpreTM and NpreTM, derived from the membrane-proximal external region (MPER) of the HIV fusion glycoprotein gp41subunit (28). According to the ANTS/DPX requenching assay, the peptides CpreTM and NpreTM exhibit all-or-none and graded behavior, respectively (21). It has been proposed that the membrane-perturbing properties of the MPER domain of HIV-1 gp41 are required for Env fusogenic function (29,30). Evidence that anti-gp41 HIV neutralizing antibodies recognize MPER epitopes and block its lytic activity in vitro adds support to this idea and suggests that this domain's function may provide a new target in the development of antiviral therapies (31,32). This is why the investigation of the mechanism of action of these peptides deserves special attention.

Our results indicate that the all-or-none CpreTM peptide induces total filling of the individual vesicles associated with long-lived membrane permeabilization, which occurs very rapidly once it starts. In contrast, the graded NpreTM peptide induces unstable permeabilization characterized by slower kinetics of dye entry, which lead to partial filling of the individual vesicles. Of importance, we show that the presence of cholesterol (Chol) in the lipid bilayer increases the number of vesicles bearing stably opened pores. This Chol effect could reflect an adaptation of the gp41 MPER sequences to inducing perturbations of the Chol-enriched viral membrane integrity. In addition, our single-vesicle approach allows one to distinguish mixed mechanisms within the same sample. Specifically, we detect a vesicle fraction permeabilized by NpreTM following an all-or-none mechanism, and GUV subpopulations, among the CpreTM-treated vesicles, characterized by transient or permanent states of permeabilization. This feature proved essential for elucidating how Chol affects membrane permeabilization by CpreTM and NpreTM. To our best knowledge, this work presents the first clear demonstration of graded and all-or-none release by fluorescence microscopy. Overall, our results both agree with and expand the mechanistic information inferred from determination by the ANTS/DPX requenching assay.

MATERIALS AND METHODS

Materials

The MPER-derived NEQELLELDKWASLWNWFNITNWLWYIK (NpreTM) and KKKNWFDITNWLWYIKLFIMIVGGLVKK (CpreTM) peptides and rhodamine-labeled fluorescent derivatives were produced by solid-phase synthesis using Fmoc chemistry as C-terminal carboxamides, and purified by high-performance liquid chromatography in the Proteomics Unit of the University Pompeu-Fabra (Barcelona, Spain). Peptide stock solutions were prepared in dimethylsulfoxide (spectroscopy grade) and the concentrations were determined using a bicinchoninic acid microassay (Pierce, Rockford, IL). 1-Palmitoyl-2-oleoylphosphatidylcholine (POPC) and Chol were purchased from Avanti Polar Lipids (Alabaster, AL). 1,19-Dioctadecyl-3,3,39,39-tetramethylindodicarbocyanine perchlorate (DiD), 1,1′-dioctadecyl-3,3′-oxacarbocyanine perchlorate (DiO), and Alexa Fluor 488 and 555 fluorescent probes were obtained from Molecular Probes (Eugene, OR).

LUV permeabilization mechanism

We determined the leakage mechanism in LUVs using the ANTS/DPX requenching assay as described previously (14,18,19,21,33). The goal of this assay is to establish the dependence of the quenching inside vesicles (Q_{in}) on the ANTS fraction outside vesicles (f_{out}). Q_{in} is defined as the ratio between the ANTS fluorescence inside vesicles at any time (F_i) and its maximum possible value in the absence of DPX (F_{imax}). Q_{in} remains constant and low for any f_{out} value when peptide-induced leakage follows an all-or-none mechanism, i.e., the population of vesicles consists of those that did not leak at all and those that released all of their aqueous contents. An increase of Q_{in} as a function of f_{out} reveals a dilution of both quencher and probe in the lumen of the vesicles, indicating that the leakage mechanism is graded, in which case the vesicles lose some of their contents.

Preparation of GUVs

GUVs of the desired lipid composition were prepared according to the electroformation method as described previously (23). Briefly, 5 μL of POPC or POPC/Chol 4:1 (mol/mol) at 1 mg/mL were spread on platinum wires. After the solvent evaporated, electroformation proceeded at 2.4 V, 10 Hz, at room temperature for 2 h in 350 μL of a 300 mM sucrose solution. An extra half an hour at 2 Hz is needed to ensure proper detachment of the GUVs from the wires. A fraction of the solution (typically 50 μL) was transferred to 500 μL of phosphate-buffered saline (PBS) in a Lab-Tek eight-chambered No. 1.0 borosilicate coverglass (Nalge Nunc International, Rochester, NY) that was previously blocked with 2 mg/mL bovine serum albumin for confocal microscopy analyses.

Confocal microscopy

Confocal fluorescence microscopy of GUVs was performed on a commercial LSM510 system (Zeiss, Jena, Germany) with a laser scanning module in multitrack mode. The excitation light from an Ar ion laser at 488 nm, an He-Ne laser at 543 nm, or an He-Ne laser at 633 nm was reflected by a dichroic mirror (HFT UV/488/543/633) and focused through a Zeiss C-Apochromat 40×, numerical aperture 1.2, water immersion objective onto the sample. The pinhole size was set to 90 μm in the green channel and adjusted in the red channel for the same z thickness. Emitted fluorescence was separated with a secondary dichroic beam splitter (NFT 545) and collected with photomultiplier detectors after passage through a 505–530 nm bandpass filter for emissions of molecules excited at 488 nm (first channel) or a 650 nm long pass filter for molecules excited at 633 nm (second channel). When an excitation laser at 543 nm was used, a second track was configured with a 560 nm long pass filter. Image processing and analyses were carried out with ImageJ (http://rsb.info.nih.gov/ij/).

Membrane permeabilization

Permeabilization measurements were obtained as previously described (23,24) by adding the GUVs to a previously stirred PBS solution containing free Alexa Fluor 488 as a marker and the lytic peptide at the desired concentration (typically 0.2 μM). The sample was gently mixed to achieve a largely homogeneous distribution of vesicles, marker, and peptide. The degree of vesicle permeabilization (filling kinetics) was determined by collecting pictures of several GUVs in different samples every 10 s for 1 h. To obtain the final extents of vesicle permeabilization, pictures of several regions of the sample were taken after 2 h of incubation of the GUV with or without the peptide. To measure the stability of the permeabilization, 5 h after treatment of GUV with the peptides in the presence of free Alexa488, a second marker, free Alexa555, was added and additional pictures of several regions of the sample were taken.

RESULTS AND DISCUSSION

CpreTM and NpreTM induce permeabilization of LUVs following different mechanisms

CpreTM and NpreTM are membrane-active peptides derived from the MPER region of the HIV fusion protein gp41 (for a scheme, see Fig. S1 in the Supporting Material). For comparison, we first characterized the membrane permeabilization mechanisms of these peptides in bulk experiments using LUVs (Fig. 1). The ANTS requenching data obtained are consistent with CpreTM and NpreTM-induced LUV permeabilization obeying all-or-none and graded mechanisms, respectively (21).

Fig. 1 also compares the mechanisms of POPC and POPC/Chol 4:1 LUV permeabilization by the peptides. Selection of the POPC/Chol 4:1 composition for comparison was done on the following basis: Chol is a relatively important constituent of the HIV-1 lipid envelope (34), which modulates MPER membrane activity (29,32). However, this lipid acts against the membrane deformation required for peptide insertion, and thus has been proposed to inhibit partitioning of peptides into the membrane interface (35). We found empirically that the partitioning capacities of MPER peptides into POPC vesicles were unaffected by including Chol in the 0–20 mol % range, but reduced when present at higher concentrations (data not shown). In

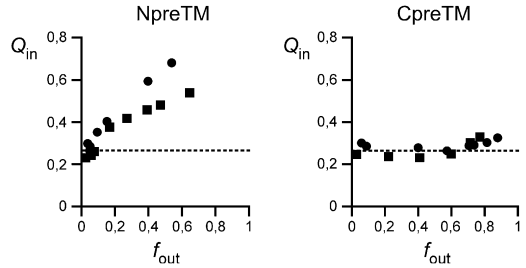

FIGURE 1 MPER-derived NpreTM and CpreTM peptides permeabilize LUVs following distinct mechanisms. Fluorescence requenching assays were carried out to establish the mechanism of membrane permeabilization in POPC and POPC/Chol 4:1 vesicles (*circles* and *squares*, respectively). Internal quenching (Q_{in}) was measured as a function of the ANTS released (f_{out}) after incubation for 60 min with peptides in a range of concentrations allowing final leakage extents below 100%. To determine these parameters, we followed the methodology of Ladokhin et al. (18,19). The horizontal dashed lines denote the expected behavior for all-or-none processes.

line with this observation, the onset value for the elastic modulus increase induced by Chol in binary mixtures with PC lies between 15 and 20 mol % (E. Evans, Biomedical Engineering, Boston University, personal communication, 2010). Thus, the change observed in the NpreTM-induced permeabilization mechanism upon inclusion of Chol (Fig. 1) is not due to a variation in the peptide membrane load. This change is reflected as the reduction of measured Q_{in} as a function of f_{out}. As discussed previously for graded mechanisms, changes in the slopes might be caused by a preferential release of ANTS or DPX, a coexisting fraction of vesicles following an all-or-none mechanism, or a combination of both (18). As a consequence, differentiating between these possibilities by means of the requenching method is in principle not practical.

In summary, the MPER-derived peptides provide a good model for performing a comparative analysis of all-or-none versus graded permeabilization mechanisms in single vesicles, and characterizing the effects exerted by a relevant lipid on those mechanisms. The main goal of such an approach is to more precisely define the distinct features underlying both mechanisms at the single-vesicle level.

CpreTM and NpreTM induce the permeabilization of individual vesicles with distinct kinetics

To follow the permeabilization kinetics of single GUVs, we added the vesicles into a solution containing the corresponding peptide and free Alexa488. We followed the entry of the fluorescent dye into the GUVs, which were initially devoid of it, by time-lapse confocal microscopy for 1 h (Fig. 2, *A* and *B*, Movie S1, and Movie S2). Simultaneously with dye entry, we observed that the integrity of the vesicles was maintained during the permeabilization process. In these experiments, we used concentrations of peptides that typically caused permeabilization of 60–80% of the vesicles under our experimental conditions. In this way, we avoided

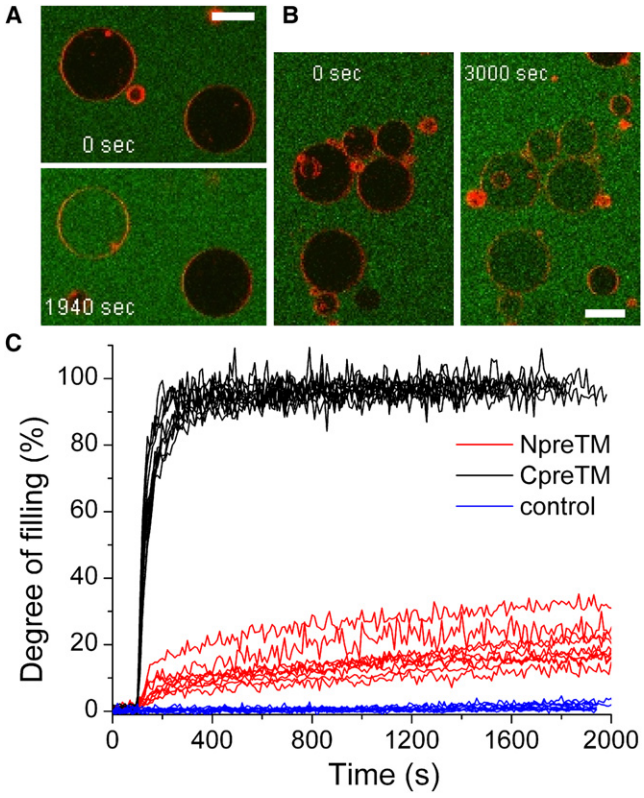

FIGURE 2 CpreTM and NpreTM show different kinetics of single-vesicle filling during permeabilization. (*A* and *B*) GUVs (*red*) in a solution containing free Alexa488 (*green*) at the indicated time points after addition of CpreTM (*A*) or NpreTM (*B*). Scale bars: 15 μm. (*C*) Kinetics of single-vesicle permeabilization by CpreTM (*black lines*) and NpreTM (*red lines*). Control vesicles are shown in blue. For clarity in the comparison, the starting points of dye influx have been aligned. In all cases, GUVs were composed of POPC 0.1% DiD and the peptide concentration was 0.5 μM.

working under saturation and were able to set reference conditions for comparison with bulk assays.

We quantified the kinetics of vesicle permeabilization by averaging the fluorescence intensity inside a single GUV at different time points and normalizing it with respect to the external fluorescence (Fig. 2 *C*). Of interest, after mixing with the peptides, dye influx due to membrane permeabilization started at different lag times (between 0 and 20 min) for each individual vesicle for both peptides. This reflects the stochastic nature of the process of membrane permeabilization. Comparable behavior was previously reported for similar systems (24,25,36). As shown in Fig. 2 *C*, the kinetics of dye entry induced by CpreTM or NpreTM exhibited very different characteristics. It is important to note that, to simplify the comparisons, we aligned the fluorescence traces with respect to the starting point. Permeabilization by CpreTM was fast (initial filling rate 2.1 $\pm$ 0.6% $\times$ s^{-1}, $n = 10$) and reached 80% ~100 s after it started. In contrast, fluorescence inside the vesicles in the presence of NpreTM increased gradually and did not reach equilibrium with the external medium (i.e.,, 100% filling) during the observation time. The filling kinetics was much slower and more heterogeneous than with CpretM and usually exhibited two regimes: the rate of dye entry started at 0.10 $\pm$ 0.06% $\times$ s^{-1} ($n = 24$) and it attenuated after ~100–200 s. Such differences in behavior are reminiscent of the different mechanisms of action of the peptides, classified as all-or-none for CpreTM and graded in the case of NpreTM.

As a control to check that vesicle permeabilization by the peptides was actually accompanied by membrane binding, we used fluorescently labeled versions of the peptides. Fig. 3 shows that peptide fluorescence in GUVs of the same lipid composition was similar for both peptides, qualitatively indicating that binding of CpreTM and NpreTM was comparable. The distribution of the fluorescent peptides was homogeneous and we did not detect peptide aggregates on the membrane that could have effects on its permeability.

It is important to note that our single-vesicle analysis of the influx kinetics demonstrates fundamental differences

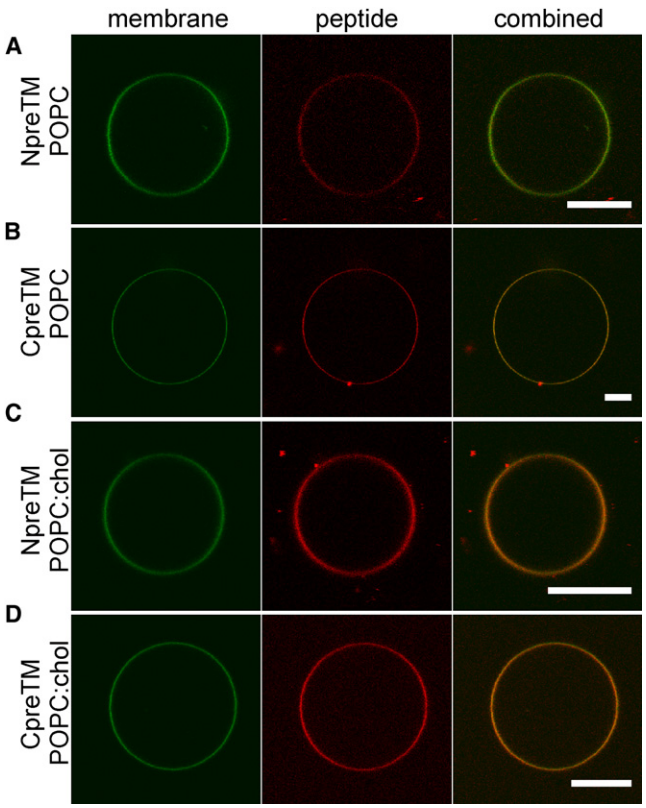

FIGURE 3 Binding of fluorescently labeled NpreTM and CpreTM peptides to GUVs is homogeneous and comparable. (*A* and *C*) NpreTM-rhodamine binding to GUVs composed of POPC (*A*) or POPC/Chol (4:1) (*C*) and containing 0.1% DiO. (*B* and *D*) CpreTM-rhodamine binding to GUVs composed of POPC (*B*) or POPC/Chol (4:1) (*D*) and containing 0.1% DiO. The panels in the first column show the DiO-labeled GUVs, the panels in the second column show the corresponding rhodamine-labeled peptide, and the panels in the third column correspond to the combination of the first two (4 μM concentration of fluorescent peptides in the external solution, 1 h incubation time). Scale bars: 15 μm.

in the nature of the permeabilization process of the all-or-none and graded models. In the case of CpreTM, even after peptide binding, the lipid membrane remains impermeable until a certain moment when there is a fast transition into a permeated state. The fast influx observed for this permeated state is likely associated with the simultaneous (at least in the time resolution of our experiments) opening of many pores or a relatively large, very efficient pore (7). This indicates that the all-or-none mechanism of membrane permeabilization is linked to some kind of cooperative transition from a closed to an open pore state, as in the two-state model proposed by Huang (37). However, in the case of the graded influx kinetics induced by NpreTM, the alteration of the bilayer permeability is carried out by smaller and/or short-lived structures that do not allow rapid filling of the vesicle. With respect to bulk experiments, the influx time of a single vesicle is now comparable to that of the vesicle population, and it reflects the duration and/or size of the membrane perturbation (7).

Single-vesicle quantification of the degree of filling: all-or-none versus graded

One of the most intriguing questions regarding partial release of contents in bulk leakage experiments is whether only some of the liposomes release all of their contents or all liposomes in the sample release part of their contents. The nature of the measurement precludes one from distinguishing between these possibilities. This issue can be indirectly assessed with additional ANTS/DPX requenching assays (10). Instead, however, our single-vesicle approach allowed us to simultaneously address this issue by performing direct observations and comparing the all-or-none and graded mechanisms of membrane permeabilization.

To that end, we took images of the GUVs samples after 2 h of incubation in the presence of CpreTM or NpreTM and free Alexa488. By comparing the average fluorescence intensity of Alexa488 inside the individual vesicles and in the external medium, we were able to calculate the filling degree for each single vesicle. For the statistical analysis, we sampled 200–500 vesicles in each experiment and repeated each experiment three times.

Fig. 4 *A* shows the distribution of filling degrees for the individual vesicles in the ensemble of GUVs. Of interest, these distributions looked very different when the samples were incubated with CpreTM or NpreTM. In the first case, which is associated with an all-or-none mechanism, the vesicles presented two states: they were totally filled with free dye, having reached equilibrium with the external fluorophore concentration (>80% filling), or they remained impermeable to it (<10% filling). Taking these two states into account, we conclude that ~70% of the vesicles were totally permeabilized and ~30% of the GUVs remained impermeable (Fig. 4 *A* and Fig. S2 *B*). In contrast, in the case of NpreTM, which follows a graded mechanism,

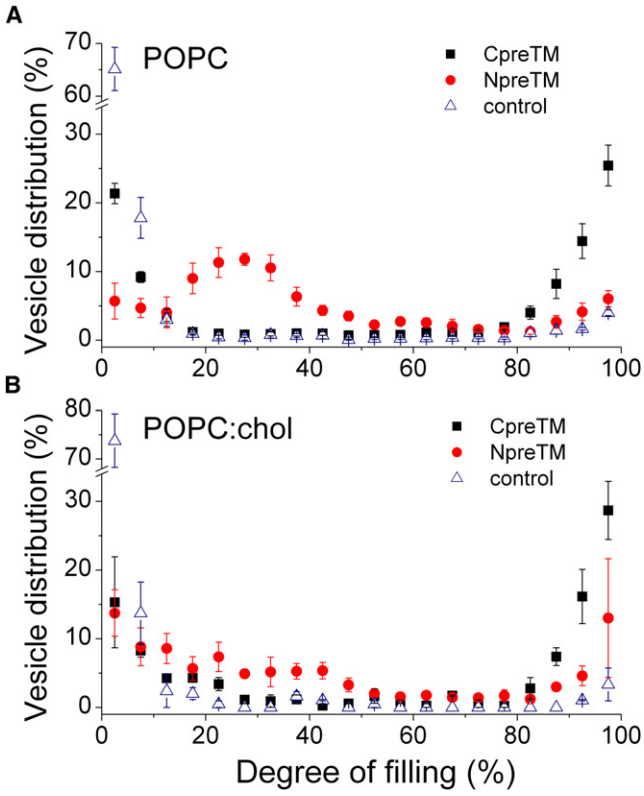

FIGURE 4 CpreTM and NpreTM induce different degrees of filling in individual vesicles. The distribution of GUVs as a function of the degree of filling after 2 h incubation with the indicated peptide (CpreTM, *squares*; NpreTM, *circles*; control, *triangles*) is shown in GUVs made of POPC 0.1% DiD (*A*) and POPC/Chol (4:1) 0.1% DiD (*B*). Error bars correspond to the relative error calculated from two (control and CpreTM) or three (NpreTM) independent experiments. Bin size is 5%.

a wide peak around 30% filling was obtained. This indicates that there is heterogeneity in the degree of filling of the individual vesicles, which in most cases is partial. Indeed, <10% of the vesicles remained impermeable and <10% of the vesicles were totally filled. This small percentage of total permeabilization is attributable to the fact that in a preparation of GUVs, ~10% of the vesicles are somehow permeable, as also observed in the control samples.

These results indicate that for individual vesicles, the degree of filling and, in analogy, the percentage of contents release differ depending on the mechanism of membrane permeabilization. The apparent 70% permeabilization in the bulk experiments implies that 70% of the vesicles are totally permeabilized for all-or-none peptides, whereas with the graded mechanism it is closer to a situation in which most vesicles have released ~70% of their contents (or have been filled to a similar degree (i.e., ~70%) depending on the nature of the experiment; Fig. 4 *A* and Fig. S2, *A* and *C*). Of importance, the single-vesicle approach also shows that in a sample of vesicles there is heterogeneity in the filling degrees at the level of the individual liposomes. And, indeed, this method also provides a means of assessing

the coexistence within the same sample of vesicle subpopulations permeabilized according to different mechanisms (see below).

Our observations also have implications for the molecular details of the permeabilization process. In the case of the all-or-none mechanism, the pore state is characterized by a sufficiently long existence to allow equilibration of the probe with the external medium. However, the permeabilization process in the graded mechanism seems to be related to smaller alterations of the bilayer permeability that do not allow rapid equilibration of contents.

CpreTM tends to form stable pores, whereas membrane permeabilization by NpreTM is transient

According to the above lines of thinking, the duration of the permeabilized state of the lipid bilayer would be different in the case of all-or-none and graded mechanisms. Recently, Fuertes et al. (16) optimized an assay to assess the long-term stability in GUVs and showed that Baxα5, a pore-forming peptide derived from Bax that follows an all-or-none mechanism, forms stable pores in equilibrium. We carried out similar experiments to qualitatively evaluate and compare the duration of the membrane permeabilization induced by CpreTM and NpreTM. In this assay, membrane permeability is measured once the peptide/membrane system has reached or is close to equilibrium. For that purpose, 5 h after incubation of the GUVs with the corresponding peptide and free Alexa488, we added a second dye: free Alexa555. We gently mixed the suspensions and imaged the samples to quantify the permeability of the GUVs to both dyes.

As shown in Fig. 5, the permeability to the second dye clearly differs between the vesicles incubated with NpreTM or CpreTM. In the first case, most of the GUVs that had partially allowed the entry of Alexa488 remained impermeable to Alexa555 (Fig. 5, *A* and *C*). However, in the presence of CpreTM, most of the liposomes that were permeable to the first dye also allowed the entrance of the second one, at least to a certain extent (Fig. 5, *B* and *D*).

These results indicate that the permeabilization of the lipid bilayer induced by NpreTM is transient, and at long incubation times, probably once equilibrium is reached in the system, the sealed nature of the vesicle is recovered. As explained above, such an alteration of membrane permeability can be explained by (at least) two structural alterations: 1), integration and/or translocation of the peptide into the bilayer, which is accompanied by lipid reorganizations that transiently allow the passage of polar molecules without evolving through a pore state; or 2), opening of a transient pore due to the asymmetric attack of the peptide that increases membrane tension when it binds to the outer leaflet of the vesicle. In the latter scenario, pore opening favors the distribution of the peptide molecules between both leaflets so that the membrane tension dissipates and allows pore closure.

In the case of CpreTM, the lipid bilayer stays in a permeabilized state also during or close to equilibrium conditions. This indicates that CpreTM is able to form a stable pore, at

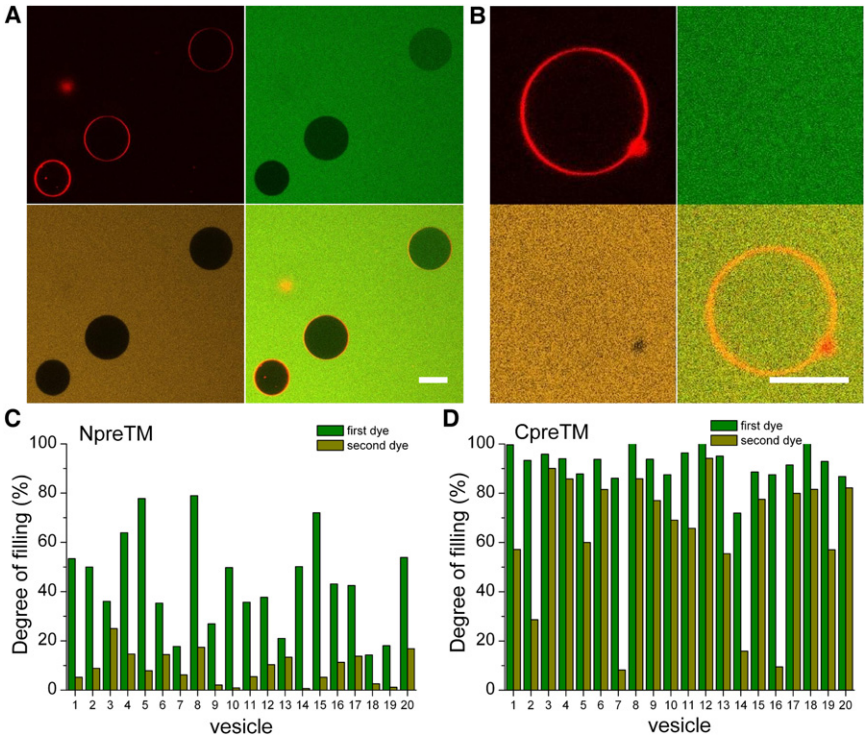

FIGURE 5 NpreTM or CpreTM induce different lifetimes of the permeabilized state in single GUVs. (*A*) GUVs in the presence of NpreTM after 5 h incubation. (*B*) GUVs in the presence of CpreTM after 5 h incubation. In *A* and B, GUVs were labeled with 0.1% DiD (*top left panel*), free Alexa488 (*top right panel*) was added simultaneously with the peptide, and free Alexa555 (*bottom left panel*) was added after the 5 h incubation. Merged images are shown in the bottom right panels. Scale bars: 10 μm. (*C* and *D*) Quantification of the degree of filling of individual GUVs with Alexa488 (*green bars*) and Alexa555 (*orange bars*) after 5 h incubation with NpreTM (*C*) and CpreTM (*D*).

least within the time frame of our experiments. Our experiments do not allow us to distinguish whether the pore is open constantly or it flickers between open and close states under equilibrium conditions; however, the consequences for membrane permeability are the same. This also means that its polypeptide sequence contains the necessary information to integrate into the lipid bilayer and adopt a structure that thermodynamically stabilizes an open pore (which otherwise is an extremely unstable event) in the membrane plane. The association of the all-or-none pore mechanism with the stabilization of a pore structure at long term and at equilibrium has been also proposed for the α5 active fragment of Bax (16). We propose that this is a general characteristic common to other all-or-none cases, such as pores formed by magainin, as opposed to the previous assumption that such pores are transiently associated with equilibration (10,38–42). As suggested by some authors and also described by dynamic simulations (36,42–44), this pore structure is probably chaotic or disorganized, with both peptide and lipid molecules lining the pore in a toroidal arrangement (41,45), i.e., the pores would be related to purely lipidic pores (9,46) but much more stable due to the presence of the peptide.

Based on the above observations, we hypothesize that graded peptides provoke membrane permeabilization only as long as the system is out of equilibrium, whereas all-or-none molecules are able to induce the opening of pores that remain in the open state once the system has reached or is close to equilibrium.

Effect of Chol on the mechanism of membrane permeabilization

Chol has been shown to play a role in the activity of gp41 (47,48). However, the detailed effects of this lipid on the HIV protein remain poorly understood. On the one hand, the MPER region of gp41 contains a CRAC domain that has been implicated in specific interactions with Chol and has been proposed to be involved in the localization of the Env protein to Chol-rich domains (49). On the other hand, several studies have shown effects of Chol on the permeabilizing and fusogenic activity of MPER peptides derived from gp41 (29). In addition, the requenching assay results shown in Fig. 1 suggest that the presence of Chol might alter the permeabilization mechanism of NpreTM. However, such a conclusion cannot be drawn from these experiments in isolation. Moreover, assuming the existence of a Chol-induced change in the graded mechanism, it is not possible to evaluate the basis of this effect from these data. To investigate possible Chol-specific effects on the action of NpreTM and CpreTM peptides from the perspective of membrane permeabilization, we applied the single-vesicle approach.

As shown in Fig. 4, *A* and *B*, the presence of Chol in the membranes of GUVs did not significantly change the distribution of vesicles according to their filling degree in the samples treated with CpreTM in comparison with pure POPC membranes. However, in the case of NpreTM, the distribution curve at ~30% filling degree decreased in height while the percentage of totally filled vesicles increased.

To perform a fine analysis of the effects of Chol, we classified the permeabilized vesicles according to the degree of entry of the first and second dyes (in experiments similar to those shown in Fig. 5, i.e., with the first dye added at time zero and the second dye added after 5 h of peptide incubation, and both dyes measured after 5 h). We arbitrarily defined a threshold by which permeabilized GUVs (>10% filling) were considered as all-or-none (filling degree of first dye > 80%) or graded (filling degree of first dye < 80%), and stable (filling degree of second dye > 80%) or unstable (filling degree of second dye < 80%). As expected from our previous observations, the number of stably permeabilized vesicles via the graded mechanism was negligible.

Although our samples were heterogeneous (mostly those containing CpreTM), the statistical analysis of the single vesicles allowed us to distinguish the effect of Chol on the permeabilizing activity of the peptides (Fig. 6, *A* and *B*). Of interest, even though the graded mechanism was still

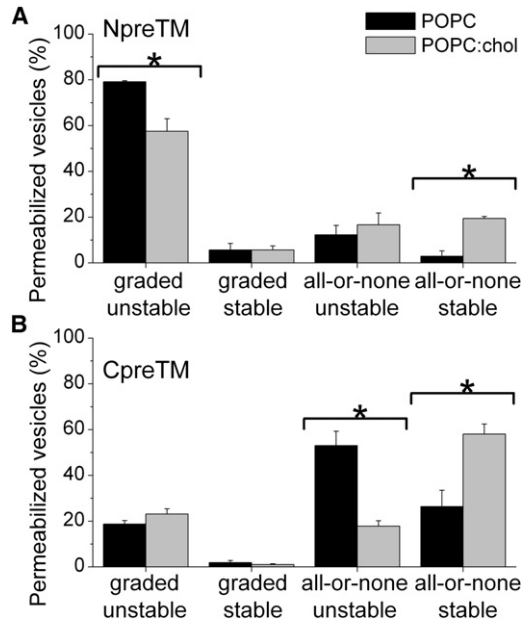

FIGURE 6 Effect of lipid composition on the mechanism of membrane permeabilization by NpreTM and CpreTM. The distributions of the mechanisms of individual GUV permeabilization by NpreTM (*A*) or CpreTM (*B*) are shown. Permeabilized GUVs (>10% filling) were classified according to their degree of filling with Alexa488 (all-or-none (>80%) versus graded (<80%)) and the lifetime of the permeabilized state (stable (permeable to Alexa555) versus unstable (impermeable to Alexa555)) after 5 h of incubation with the corresponding peptide. GUVs were composed of POPC 0.1% DiD or POPC/Chol (4:1) 0.1% DiD as indicated. Mean ± SD for the percentage values in three different samples. Chol-dependent significant changes are indicated (*$p < 0.05$).

prevalent, in the presence of Chol a significant fraction of the vesicle population was stably permeabilized by NpreTM following an all-or-none mechanism (Fig. 6 *A*). On the other hand, in the case of CpreTM, a more important effect was exerted on the lifetime of the pore state, which increased in stability when compared to pure POPC vesicles (Fig. 6 *B*).

These results show that Chol affects the permeabilizing activity of both CpreTM and NpreTM. Such an effect is likely to have functional relevance because Chol extraction inhibits virion infectivity (47). However, Chol generally has an inhibitory effect on membrane permeabilization due to the induction of negative intrinsic monolayer curvature, and it helps membrane fusion for the same reason (50). This, together with the presence of CRAC domains in the sequence of both peptides, points to a role of specific lipid/peptide interactions in the Chol effects on membrane permeabilization, as suggested by Epand and co-workers (51). Moreover, MPER lytic activity has been demonstrated to be functional in gp41-induced fusion (30). The observation made here that Chol stabilizes the membrane lytic structures induced by NpreTM and CpreTM peptides supports the notion that gp41 MPER plays an active role in generating the stresses required to fuse the viral envelope. Thus, transient membrane rupture, promotion of changes in spontaneous curvature, and even the creation of holes within membranes are all common effects proposed to underlie pore formation and fusion (52,53), which conceivably could be promoted by MPER and boosted by the high Chol content present in the viral envelope.

In a more general sense, this study also shows the extent to which lipid composition can play a role in the permeabilization process induced by membrane active peptides (46). The observation that the mechanism of membrane permeabilization of a given PFP is affected by the lipid composition suggests an effect on target membrane specificity, which is essential for the action of antimicrobial peptides, among other things (12). In this context, our single-vesicle approach allowed us to discern the detailed effects of lipid composition on the process of permeabilization of the lipid bilayer by CpreTM and NpreTM. This was possible because we were able to distinguish and quantify the coexistence of various permeabilization mechanisms in the population of liposomes, which will very likely prove relevant for enhancing our understanding of membrane permeabilization by other PFPs.

CONCLUSIONS

In this work, we used a single-vesicle approach to compare in detail two alternative mechanisms of membrane permeabilization. To that end, we chose two peptides derived from the MPER region of the HIV fusion protein gp41: CpreTM, which follows an all-or-none mechanism, and NpreTM, which permeabilizes membranes in a graded manner. A comparison of permeabilization kinetics and the distributions of the filling degrees of the individual vesicles showed that CpreTM provoked a rapid and total filling, whereas NpreTM induced slower dye entrance that ended up in a partial filling of the liposomes. Single-GUV analyses of dye entry after long incubation times also showed that the all-or-none mechanism was usually accompanied by the formation of a long-lived permeabilized state in a fraction of the vesicles. On the other hand, the graded permeabilization was transient and the membrane recovered its impermeability once equilibrium was reached. Of importance, using the single-vesicle approach we were able to quantitatively estimate vesicle fractions that were permeabilized following alternative mechanisms within the same sample. We found that the presence of Chol correlated with induction by NpreTM of all-or-none/stable leakage in a significant fraction of the vesicles, and a significant increase in the number of vesicles with stably opened CpreTM pores. Thus, we conclude that in both cases Chol affected the peptide-induced membrane permeabilization by increasing the number of stably opened pores. This finding supports the involvement of lipids in the mechanism of pore assembly, which has particular implications for the fusogenic activity of gp41. In summary, our strategy allowed us to find differences at the individual-vesicle level in the kinetics, degree, and stability of membrane permeabilization associated with all-or-none and graded mechanisms.

SUPPORTING MATERIAL

Three figures and two movies are available at http://www.biophysj.org/biophysj/supplemental/S0006-3495(10)01174-4.

We thank J. Salgado and G. Fuertes for useful discussions.

This study was supported by the Max Planck Society (A.J.G.-S.), the Ministerio de Ciencia e Innovación (BIO2008-00772), and the University of the Basque Country (GIU 06/42 and DIPE08/12 to J.L.N.). B.A. was the recipient of a predoctoral Ministerio de Educación y Cultura-Formación del Profesorado Universitario fellowship.

REFERENCES

1. Mulkidjanian, A. Y., M. Y. Galperin, and E. V. Koonin. 2009. Co-evolution of primordial membranes and membrane proteins. *Trends Biochem. Sci.* 34:206–215.
2. Malsam, J., S. Kreye, and T. H. Söllner. 2008. Membrane fusion: SNAREs and regulation. *Cell. Mol. Life Sci.* 65:2814–2832.
3. Antignani, A., and R. J. Youle. 2006. How do Bax and Bak lead to permeabilization of the outer mitochondrial membrane? *Curr. Opin. Cell Biol.* 18:685–689.
4. Anderluh, G., and J. H. Lakey. 2008. Disparate proteins use similar architectures to damage membranes. *Trends Biochem. Sci.* 33:482–490.
5. Mathew, M., and R. S. Verma. 2009. Humanized immunotoxins: a new generation of immunotoxins for targeted cancer therapy. *Cancer Sci.* 100:1359–1365.
6. Pálffy, R., R. Gardlík, …, P. Celec. 2009. On the physiology and pathophysiology of antimicrobial peptides. *Mol. Med.* 15:51–59.

7. Almeida, P. F., and A. Pokorny. 2009. Mechanisms of antimicrobial, cytolytic, and cell-penetrating peptides: from kinetics to thermodynamics. *Biochemistry.* 48:8083–8093.
8. Huang, H. W. 2006. Molecular mechanism of antimicrobial peptides: the origin of cooperativity. *Biochim. Biophys. Acta.* 1758:1292–1302.
9. Huang, H. W., F. Y. Chen, and M. T. Lee. 2004. Molecular mechanism of peptide-induced pores in membranes. *Phys. Rev. Lett.* 92:198304.
10. Gregory, S. M., A. Pokorny, and P. F. Almeida. 2009. Magainin 2 revisited: a test of the quantitative model for the all-or-none permeabilization of phospholipid vesicles. *Biophys. J.* 96:116–131.
11. Gregory, S. M., A. Cavenaugh, …, P. F. Almeida. 2008. A quantitative model for the all-or-none permeabilization of phospholipid vesicles by the antimicrobial peptide cecropin A. *Biophys. J.* 94:1667–1680.
12. Huang, H. W. 2009. Free energies of molecular bound states in lipid bilayers: lethal concentrations of antimicrobial peptides. *Biophys. J.* 96:3263–3272.
13. Melo, M. N., R. Ferre, and M. A. Castanho. 2009. Antimicrobial peptides: linking partition, activity and high membrane-bound concentrations. *Nat. Rev. Microbiol.* 7:245–250.
14. Wimley, W. C., M. E. Selsted, and S. H. White. 1994. Interactions between human defensins and lipid bilayers: evidence for formation of multimeric pores. *Protein Sci.* 3:1362–1373.
15. García-Sáez, A. J., M. Coraiola, …, J. Salgado. 2006. Peptides corresponding to helices 5 and 6 of Bax can independently form large lipid pores. *FEBS J.* 273:971–981.
16. Fuertes, G., A. J. García-Sáez, …, J. Salgado. 2010. Pores formed by Baxα5 relax to a smaller size and keep at equilibrium. *Biophys. J.* 99:2917–2925.
17. Pokorny, A., and P. F. F. Almeida. 2004. Kinetics of dye efflux and lipid flip-flop induced by δ-lysin in phosphatidylcholine vesicles and the mechanism of graded release by amphipathic, α-helical peptides. *Biochemistry.* 43:8846–8857.
18. Ladokhin, A. S., W. C. Wimley, …, S. H. White. 1997. Mechanism of leakage of contents of membrane vesicles determined by fluorescence requenching. *Methods Enzymol.* 278:474–486.
19. Ladokhin, A. S., W. C. Wimley, and S. H. White. 1995. Leakage of membrane vesicle contents: determination of mechanism using fluorescence requenching. *Biophys. J.* 69:1964–1971.
20. Fiser, R., and I. Konopásek. 2009. Different modes of membrane permeabilization by two RTX toxins: HlyA from *Escherichia coli* and CyaA from *Bordetella pertussis*. *Biochim. Biophys. Acta.* 1788: 1249–1254.
21. Apellániz, B., S. Nir, and J. L. Nieva. 2009. Distinct mechanisms of lipid bilayer perturbation induced by peptides derived from the membrane-proximal external region of HIV-1 gp41. *Biochemistry.* 48:5320–5331.
22. Patel, H., C. Tscheka, and H. Heerklotz. 2009. Characterizing vesicle leakage by fluorescence lifetime measurements. *Soft Matter.* 5:2849–2851.
23. García-Sáez, A. J., J. Ries, …, P. Schwille. 2009. Membrane promotes tBID interaction with BCL(XL). *Nat. Struct. Mol. Biol.* 16:1178–1185.
24. Schön, P., A. J. García-Sáez, …, P. Schwille. 2008. Equinatoxin II permeabilizing activity depends on the presence of sphingomyelin and lipid phase coexistence. *Biophys. J.* 95:691–698.
25. Tamba, Y., and M. Yamazaki. 2005. Single giant unilamellar vesicle method reveals effect of antimicrobial peptide magainin 2 on membrane permeability. *Biochemistry.* 44:15823–15833.
26. Sun, Y., W. C. Hung, …, H. W. Huang. 2009. Interaction of tea catechin (−)-epigallocatechin gallate with lipid bilayers. *Biophys. J.* 96:1026–1035.
27. Ambroggio, E. E., F. Separovic, …, L. A. Bagatolli. 2005. Direct visualization of membrane leakage induced by the antibiotic peptides: maculatin, citropin, and aurein. *Biophys. J.* 89:1874–1881.
28. Montero, M., N. E. van Houten, …, J. K. Scott. 2008. The membrane-proximal external region of the human immunodeficiency virus type 1 envelope: dominant site of antibody neutralization and target for vaccine design. *Microbiol. Mol. Biol. Rev.* 72:54–84. (table of contents.).
29. Lorizate, M., N. Huarte, …, J. L. Nieva. 2008. Interfacial pre-transmembrane domains in viral proteins promoting membrane fusion and fission. *Biochim. Biophys. Acta.* 1778:1624–1639.
30. Vishwanathan, S. A., and E. Hunter. 2008. Importance of the membrane-perturbing properties of the membrane-proximal external region of human immunodeficiency virus type 1 gp41 to viral fusion. *J. Virol.* 82:5118–5126.
31. Huarte, N., M. Lorizate, …, J. L. Nieva. 2008. The broadly neutralizing anti-human immunodeficiency virus type 1 4E10 monoclonal antibody is better adapted to membrane-bound epitope recognition and blocking than 2F5. *J. Virol.* 82:8986–8996.
32. Lorizate, M., A. Cruz, …, J. L. Nieva. 2006. Recognition and blocking of HIV-1 gp41 pre-transmembrane sequence by monoclonal 4E10 antibody in a Raft-like membrane environment. *J. Biol. Chem.* 281:39598–39606.
33. Rausch, J. M., J. R. Marks, …, W. C. Wimley. 2007. β-Sheet pore-forming peptides selected from a rational combinatorial library: mechanism of pore formation in lipid vesicles and activity in biological membranes. *Biochemistry.* 46:12124–12139.
34. Aloia, R. C., H. Tian, and F. C. Jensen. 1993. Lipid composition and fluidity of the human immunodeficiency virus envelope and host cell plasma membranes. *Proc. Natl. Acad. Sci. USA.* 90:5181–5185.
35. Allende, D., S. A. Simon, and T. J. McIntosh. 2005. Melittin-induced bilayer leakage depends on lipid material properties: evidence for toroidal pores. *Biophys. J.* 88:1828–1837.
36. Tamba, Y., and M. Yamazaki. 2009. Magainin 2-induced pore formation in the lipid membranes depends on its concentration in the membrane interface. *J. Phys. Chem. B.* 113:4846–4852.
37. Huang, H. W. 2000. Action of antimicrobial peptides: two-state model. *Biochemistry.* 39:8347–8352.
38. Matsuzaki, K., O. Murase, …, K. Miyajima. 1995. Translocation of a channel-forming antimicrobial peptide, magainin 2, across lipid bilayers by forming a pore. *Biochemistry.* 34:6521–6526.
39. Rathinakumar, R., and W. C. Wimley. 2008. Biomolecular engineering by combinatorial design and high-throughput screening: small, soluble peptides that permeabilize membranes. *J. Am. Chem. Soc.* 130:9849–9858.
40. Rex, S., and G. Schwarz. 1998. Quantitative studies on the melittin-induced leakage mechanism of lipid vesicles. *Biochemistry.* 37: 2336–2345.
41. Matsuzaki, K., O. Murase, …, K. Miyajima. 1996. An antimicrobial peptide, magainin 2, induced rapid flip-flop of phospholipids coupled with pore formation and peptide translocation. *Biochemistry.* 35:11361–11368.
42. Sengupta, D., H. Leontiadou, …, S. J. Marrink. 2008. Toroidal pores formed by antimicrobial peptides show significant disorder. *Biochim. Biophys. Acta.* 1778:2308–2317.
43. Lee, M. T., W. C. Hung, …, H. W. Huang. 2008. Mechanism and kinetics of pore formation in membranes by water-soluble amphipathic peptides. *Proc. Natl. Acad. Sci. USA.* 105:5087–5092.
44. Leontiadou, H., A. E. Mark, and S. J. Marrink. 2006. Antimicrobial peptides in action. *J. Am. Chem. Soc.* 128:12156–12161.
45. Ludtke, S. J., K. He, …, H. W. Huang. 1996. Membrane pores induced by magainin. *Biochemistry.* 35:13723–13728.
46. Fuertes, G., D. Giménez, …, J. Salgado. 2010. Role of membrane lipids for the activity of pore forming peptides and proteins. *In* Proteins: Membrane Binding and Pore Formation. G. Anderluh, and J. Lakey, editors. Landes Bioscience and Springer Bioscience+Business Media.
47. Graham, D. R., E. Chertova, …, J. E. Hildreth. 2003. Cholesterol depletion of human immunodeficiency virus type 1 and simian immunodeficiency virus with β-cyclodextrin inactivates and permeabilizes the virions: evidence for virion-associated lipid rafts. *J. Virol.* 77: 8237–8248.

48. Epand, R. F., A. Thomas, …, R. M. Epand. 2006. Juxtamembrane protein segments that contribute to recruitment of cholesterol into domains. *Biochemistry.* 45:6105–6114.

49. Epand, R. F., B. G. Sayer, and R. M. Epand. 2005. The tryptophan-rich region of HIV gp41 and the promotion of cholesterol-rich domains. *Biochemistry.* 44:5525–5531.

50. Chernomordik, L. V., and J. Zimmerberg. 1995. Bending membranes to the task: structural intermediates in bilayer fusion. *Curr. Opin. Struct. Biol.* 5:541–547.

51. Epand, R. M., A. Thomas, …, R. F. Epand. 2010. Cholesterol interaction with proteins that partition into membrane domains: an overview. *Subcell. Biochem.* 51:253–278.

52. Chernomordik, L. V., and M. M. Kozlov. 2008. Mechanics of membrane fusion. *Nat. Struct. Mol. Biol.* 15:675–683.

53. Müller, M., K. Katsov, and M. Schick. 2003. A new mechanism of model membrane fusion determined from Monte Carlo simulation. *Biophys. J.* 85:1611–1623.